

# 1 CRISPR-DecrypTr reveals cis-regulatory elements from noncoding 2 perturbation screens

3  
4

5 Anders Rasmussen<sup>1,\*</sup>, Tarmo Äijö<sup>1,\*</sup>, Mariano Ignacio Gabitto<sup>1</sup>, Nicholas Carriero<sup>3</sup>, Neville  
6 Sanjana<sup>4</sup>, Jane Skok<sup>5</sup>, Richard Bonneau<sup>1,2,5,\*\*</sup>

7  
8

<sup>1</sup>Center for Computational Biology, Flatiron Institute, Simons Foundation, New York, NY 10010, USA.

9

<sup>2</sup>New York University, Center for Data Science, New York, NY 10010, USA.

10

<sup>3</sup>Scientific Computing Core, Flatiron Institute, Simons Foundation, New York, NY, 10010, USA.

11

<sup>4</sup>New York Genome Center, New York, NY, 10013, USA.

12

<sup>5</sup>New York University, Department of Biology, New York, NY 10012, USA

13

\* These authors contributed equally to this work

14

\*\* To whom correspondence should be addressed

15

16

17

18

## **Abstract:**

19

20

Clustered Regularly Interspace Short Palindromic Repeats (CRISPR)-Cas9 genome editing

21

methods provide the tools necessary to examine phenotypic impacts of targeted perturbations

22

in high-throughput screens. While these technologies have the potential to reveal functional

23

elements with direct therapeutic applications, statistical techniques to analyze noncoding

24

screen data remain limited. We present CRISPR-DecrypTr, a computational tool for the analysis

25

of CRISPR noncoding screens. Our method leverages experimental design: accounting for

26

multiple conditions, controls, and replicates to infer the regulatory landscape of noncoding

27

genomic regions. We validate our method on a variety of mutagenesis, CRISPR activation, and

28

CRISPR interference screens, extracting new insights from previously published data.

29 **Main:**

30

31

32

33

34

35

36

37

38

39

40

41

42

43

44

45

46

47

48

49

50

51

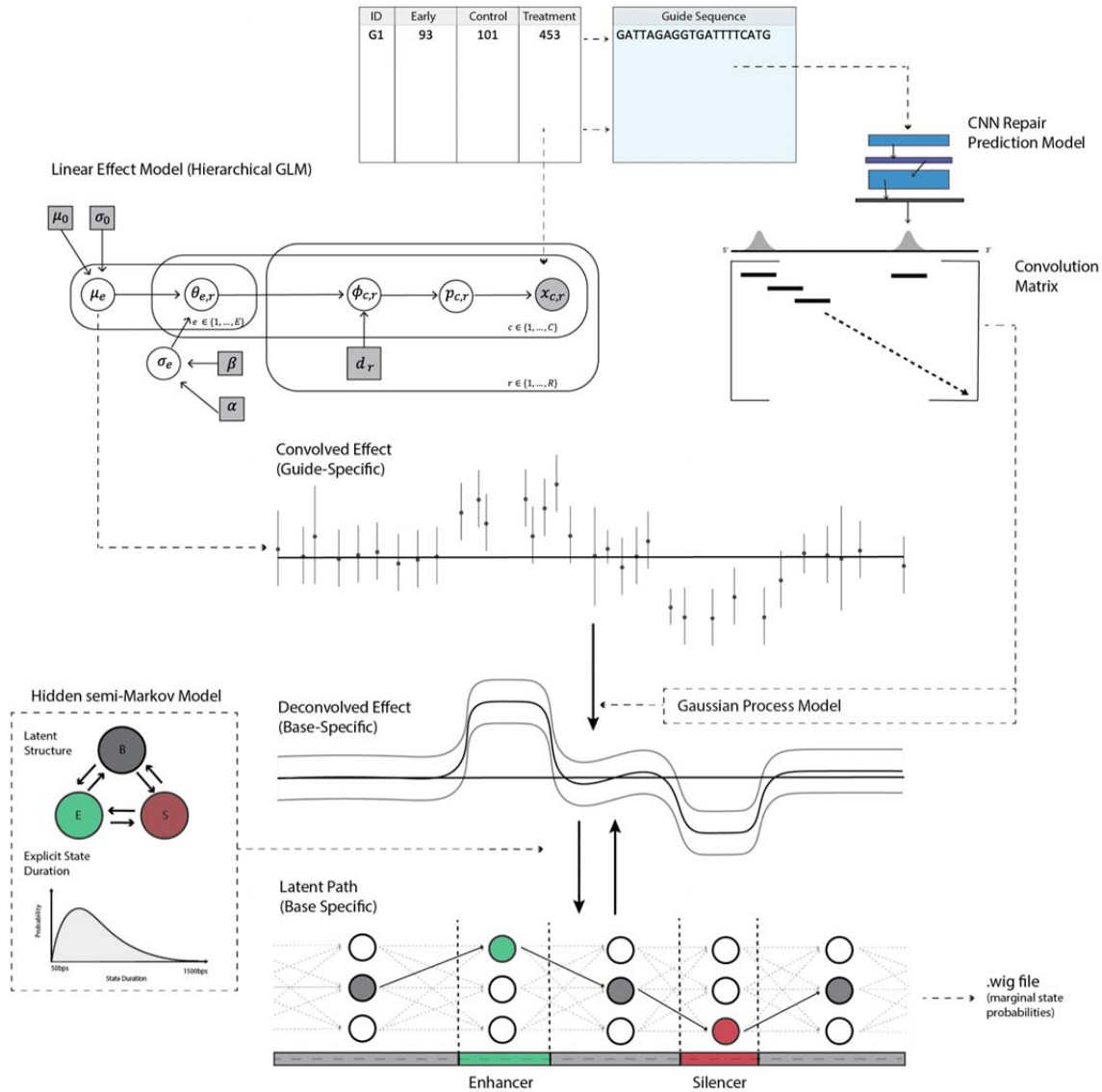
Information garnered from pooled CRISPR perturbation screens impacts decisions that have therapeutic implications. Genome-wide knockout and noncoding screens have been used to identify new therapeutic targets, to reveal genes responsible for anti-cancer drug resistance, and to map functional elements in leukemia cell lines.<sup>1,2,3,4</sup> As researchers in academia and industry make greater use of improving gene editing technologies, computational approaches that tackle the unique challenges posed by their experimental design are of increasing importance. Methods employed for knockout screens are designed to assess the impact of perturbing a genome-wide set of pre-delineated coding regions.<sup>5,6</sup> However, analysis of CRISPR noncoding screens, which employ saturated guide libraries to reveal *cis*-regulatory elements, necessitate distinct experimental considerations. Most importantly, classification of functional elements without *a priori* knowledge of their location or size requires integrating information across perturbations within genomic proximity, an aspect that renders existing knockout methods inapplicable to these experimental designs. Literature on methods for analyzing noncoding screens is scarce, with only a single method published that addresses one of the many aspects of noncoding screen analysis.<sup>7</sup>

CRISPR-DecrypTr utilizes techniques from Bayesian inference, signal processing, and latent variable models to integrate data and experimental design, allowing the end-user to make precise conclusions about their noncoding screen results (**Figure 1**; *Methods*). A Bayesian hierarchical generalized linear model (GLM) serves as the mathematical formulation from which perturbation-specific effect on phenotype are inferred<sup>8,9</sup>. The model leverages experimental

52 conditions, controls, and replicates in a single numerical procedure implemented with Markov  
53 Chain Monte Carlo, allowing for rigorous statistical treatment of parameter uncertainty  
54 (*Methods 2.2*). Effects are mapped to a base-by-base level of granularity through a Gaussian  
55 process-based model (*Methods 2.4*)<sup>10</sup>. This deconvolution fully accounts for guide-specificity,  
56 off-target effects and, if applicable, double-strand break (DSB) repair uncertainty (*Methods*  
57 *2.3*)<sup>11, 12</sup>. A hidden semi-Markov model (HsMM) incorporates spatial information to decode the  
58 latent regulatory landscape of interest, revealing enhancers and silencers in the noncoding  
59 genome (*Methods 2.5*)<sup>13</sup>. Regulatory element calls and guide-specific effects are exported in  
60 bioinformatics file formats such as Browser Extendable Data (.bed) and Wiggle (.wig) that can  
61 easily be explored in genomic visualization software such as the Integrative Genomics Viewer  
62 (IGV)<sup>14</sup>.

63

64



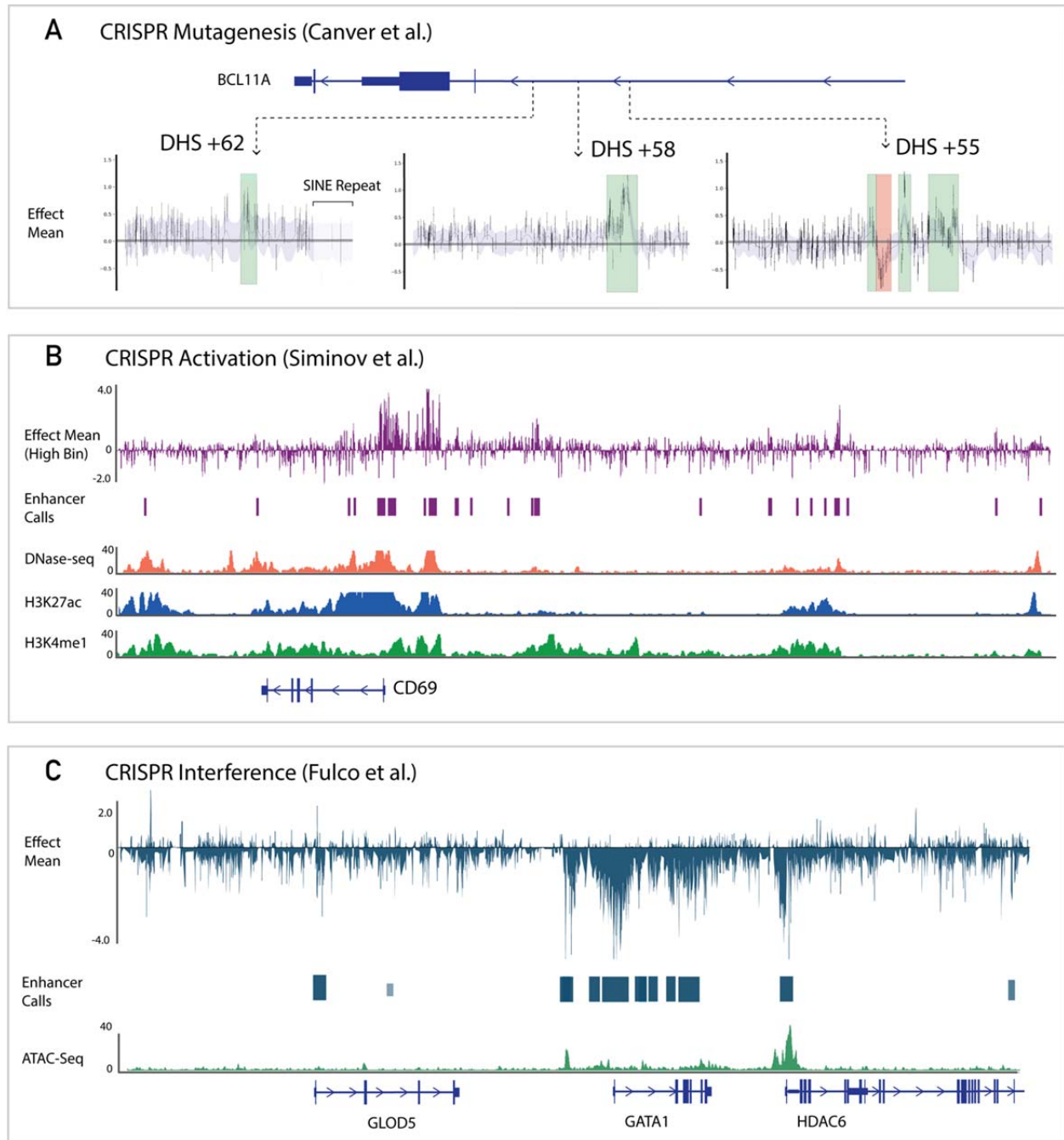
65  
66  
67  
68  
69  
70  
71  
72  
73

**Figure 1:** Overview of the CRISPR-Decryptr method for the analysis of noncoding screens. The hierarchical GLM infers perturbation-specific regulatory effect on phenotype from raw guide RNA (gRNA) counts (*top left*). Guide RNA sequences are used to construct a convolution matrix accounting for specificity, off-target effects, and repair uncertainty in the case of mutagenesis screens (*top right*). Finally, iterating between Gaussian Process deconvolution and HsMM training and prediction reveals base-specific effects and ultimately the latent state path of interest (*bottom half*).

74 We validated CRISPR-DecrypTr on noncoding screens of distinct experimental designs,  
75 including CRISPR mutagenesis, CRISPR activation (CRISPRa), and CRISPR interference (CRISPRi)  
76 screens (**Figure 2**)<sup>4, 15, 16</sup>. In the CRISPR mutagenesis screen (Canver *et al.*), three intronic DNase  
77 hypersensitivity sites (DHS) within *BCL11A* were perturbed in human umbilical cord blood-  
78 derived erythroid progenitor (HUDEP) cells<sup>15</sup>. These sites, termed DHS +62, +58, and +55, are  
79 known to impact fetal hemoglobin (HgF) levels from prior published research, with the  
80 enhancer identified in DHS +58 having proven a successful therapeutic target in two patients  
81 with hemoglobinopathies.<sup>17</sup> When applied to this dataset, CRISPR-DecrypTr produced  
82 regulatory state calls in agreement with the original analysis (**Figure 2A** and **Supplementary**  
83 **Figure 3.1.1**). The CRISPR activation screen we re-analyzed (Simionov *et al.*) targeted the *IL2RA*  
84 and *CD69* gene loci in Jurkat T-cells.<sup>16</sup> To measure phenotypic change, the FACS sort cells into a  
85 “negative”, “low”, “medium”, and “high” bins of *IL2RA* and *CD69* based on expression levels.  
86 Analysis of the two gene loci with CRISPR-DecrypTr recalls the enhancers from the original  
87 analysis, as well as novel putative enhancers that are correlated with DNase-seq and H3K27ac  
88 from the Jurkat-T Cell line (**Supplementary Figures 3.2.2** and **3.2.3**). Finally, the re-analysis of  
89 the Fulco *et al.* CRISPRi screen of the *GATA1* gene loci revealed similar regulatory element calls  
90 to the original analysis.<sup>4</sup> (**Figure 2C** and **Supplementary Figure 4.3.1**).

91 We have described a statistical technique for analyzing CRISPR noncoding screen data  
92 and illustrated the accuracy of CRISPR-DecrypTr on three distinct perturbation technologies,  
93 demonstrating the method’s ability to reveal novel insights from a diverse set of experimental  
94 designs. CRISPR-DecrypTr will be a valuable component in future attempts to identify functional

95 genomic elements and their link to phenotypic traits, enabling target identification and  
96 synthetic biology in biomedical and biotechnological settings.



97  
98 **Figure 2:** Regulatory elements classified by CRISPR-Decryptr for three published noncoding  
99 screens. **A:** Analysis mutagenesis screen targeting BCL11A DHS sites reveals similar enhancer  
100 and silencer locations as in the original publications. **B:** Analysis CRISPRa screen targeting CD69  
101 promoter region reveals novel enhancer calls. **C:** Analysis CRISPRi screen targeting GATA1 gene  
102 loci reveals the same enhancer calls as in the original analysis.

103 **Code Availability:**

104

105 CRISPR-DecrypTr code and readme are located at:

106 [https://github.com/anders-w-rasmussen/crispr\\_decryptr](https://github.com/anders-w-rasmussen/crispr_decryptr)

107

108 **Data Availability:**

109

110 All data is available at [https://github.com/anders-w-rasmussen/crispr\\_decryptr](https://github.com/anders-w-rasmussen/crispr_decryptr)

111

112 No restrictions on data are applicable here. All data used were publicly available.

113

114

115 **Acknowledgements:**

116

117 This research was made possible by the Simons Foundation. RB and MG acknowledge support

118 from the following sources: NIH R01DK103358, Simons Foundation, NSF-IOS-1546218,

119 R35GM122515, NSF CBET-1728858, and NIH R01AI130945

120

121

122 **Contributions:**

123

124 A.R. conceived of the model with guidance and oversight from R.B. and T.Ä. The inference step

125 of the method and Gaussian Process deconvolution were formulated and coded by T.Ä. Off-

126 target, repair outcome prediction, and the Gaussian Process / HsMM iterative procedure were

127 formulated by A.R. The majority of HsMM code is adapted from previous work by done by

128 M.I.G and A.R. in developing the ChromA algorithm. Rules for HsMM parameter updates and

129 variational methods were developed by M.I.G. N.C. was instrumental in advising on high-

130 performance computing considerations. N.S. and J.S. provided important insight into noncoding

131 screens from the viewpoint of experimentalists and were central in bringing the need for this

132 statistical method to A.R. and R.B.'s attention. A.R. did analyses of published data, wrote the

133 paper supplement, and wrote the CRISPR-DecrypTr software. All authors contributed to the

134 writing of the manuscript.

135

136

137 **Competing Interests:**

138

139 A.R. owns stock in Editas medicine and 10x Genomics. T.Ä. owns stock in 10x Genomics.

140

141 R.B. has ongoing or recent consulting or advisory relationships with Eli Lilly, Merus, Merck and

142 Epistemic AI.

143

144 **References:**

145 <sup>1</sup>Wei, L., Lee, D., Law, C. *et al.* Genome-wide CRISPR/Cas9 library screening identified PHGDH as  
146 a critical driver for Sorafenib resistance in HCC. *Nat Commun* **10**, 4681 (2019).

147

148 <sup>2</sup>Lau, M., Ghazanfar, S., Parkin, A. *et al.* Systematic functional identification of cancer multi-  
149 drug resistance genes. *Genome Biol* **21**, 27 (2020).

150

151 <sup>3</sup>Fellmann, C., Gowen, B., Lin, P. *et al.* Cornerstones of CRISPR–Cas in drug discovery and  
152 therapy. *Nat Rev Drug Discov* **16**, 89–100 (2017).

153

154 <sup>4</sup>Fulco, C.P, Munschauer, M. Anyoha, R. Systematic mapping of functional enhancer–promoter  
155 connections with CRISPR interference. *Science* **354**, 769–773 (2016).

156

157 <sup>5</sup>Li, W., Xu, H., Xiao, T. *et al.* MAGeCK enables robust identification of essential genes from  
158 genome-scale CRISPR/Cas9 knockout screens. *Genome Biol* **15**, 554 (2014).

159

160 <sup>6</sup>Allen, F., Khodak, A. Behan, F. *et al.* JACKS: joint analysis of CRISPR/Cas9 knockout screens.  
161 *Genome Research* **29**, 464-471 (2019)

162

163 <sup>7</sup>Hsu, J.Y., Fulco, C.P., Cole, M.A. *et al.* CRISPR-SURF: discovering regulatory elements by  
164 deconvolution of CRISPR tiling screen data. *Nat Methods* **15**, 992–993 (2018).

165

166 <sup>8</sup>Gelman A, Hill J. *Data analysis using regression and multilevel/hierarchical models* (Cambridge  
167 university press, Cambridge, 2006).

168

169 <sup>9</sup>Gelman, Andrew, *et al.* *Bayesian data analysis* (CRC press, Boca Raton, FL, 2013).

170

171 <sup>10</sup>Rasmussen, C.E., Williams, C.K. *Gaussian Processes for Machine Learning* (The MIT Press,  
172 Cambridge, MA, 2006)

173

174 <sup>11</sup>Hsu, P., Scott, D., Weinstein, J. *et al.* DNA targeting specificity of RNA-guided Cas9 nucleases.  
175 *Nat Biotechnol* **31**, 827–832 (2013).

176

177 <sup>12</sup>Allen, F., Crepaldi, L., Alsinet, C. *et al.* Predicting the mutations generated by repair of Cas9-  
178 induced double-strand breaks. *Nat Biotechnol* **37**, 64–72 (2019).

179

180 <sup>13</sup>Gabitto, M.I., Rasmussen, A., Wapinski, O. *et al.* Characterizing chromatin landscape from  
181 aggregate and single-cell genomic assays using flexible duration modeling. *Nat Commun* **11**, 747  
182 (2020).

183

184 <sup>14</sup>Robinson, J., Thorvaldsdóttir, H., Winckler, W. *et al.* Integrative genomics viewer. *Nat*  
185 *Biotechnol* **29**, 24–26 (2011).



186  
187  
188  
189  
190  
191  
192  
193  
194  
195  
196  
197  
198

<sup>15</sup> Canver, M., Smith, E., Sher, F. *et al.* *BCL11A* enhancer dissection by Cas9-mediated *in situ* saturating mutagenesis. *Nature* **527**, 192–197 (2015).

<sup>16</sup> Simeonov, D., Gowen, B., Boontanrart, M. *et al.* Discovery of stimulation-responsive immune enhancers with CRISPR activation. *Nature* **549**, 111–115 (2017).

<sup>17</sup> Bauer DE, et al. An Erythroid Enhancer of BCL11A Subject to Genetic Variation Determines Fetal Hemoglobin Level. *Science* **342**, 253–257 (2013).